DTU Library

Photonic cavity design by topology optimization

Christiansen, Rasmus E.; Wang, Fengwen; Mørk, Jesper; Sigmund, Ole

Published in:
Proceedings of SPIE - Nanoengineering: Fabrication, Properties, Optics, Thin Films, and Devices XVI

Link to article, DOI:
10.1117/12.2529099

Publication date:
2019

Document Version
Publisher's PDF, also known as Version of record

Citation (APA):
Christiansen, R. E., Wang, F., Mørk, J., & Sigmund, O. (2019). Photonic cavity design by topology optimization. In B. Panchapakesan, & A-J. Attias (Eds.), *Proceedings of SPIE - Nanoengineering: Fabrication, Properties, Optics, Thin Films, and Devices XVI* (Vol. 1189). [110890A] SPIE - International Society for Optical Engineering. Proceedings of SPIE - The International Society for Optical Engineering https://doi.org/10.1117/12.2529099

Photonic cavity design by topology optimization

Rasmus E. Christiansen, Fengwen Wang, Jesper Mørk, Ole Sigmund

Rasmus E. Christiansen, Fengwen Wang, Jesper Mørk, Ole Sigmund, "Photonic cavity design by topology optimization," Proc. SPIE 11089, Nanoengineering: Fabrication, Properties, Optics, Thin Films, and Devices XVI, 110890A (3 September 2019); doi: 10.1117/12.2529099

SPIE.

Event: SPIE Nanoscience + Engineering, 2019, San Diego, California, United States

Photonic cavity design by topology optimization

Rasmus E. Christiansen[1,*], **Fengwen Wang**[1], **Jesper Mørk**[2], **Ole Sigmund**[1]

[1] Department of Mechanical Engineering, Technical University of Denmark,
Nils Koppels Allé 404, DK-2800 Kgs. Lyngby, Denmark
[2] Department of Photonics Engineering, DTU Fotonik, Technical University of Denmark,
Building 343, DK-2800 Kgs. Lyngby, Denmark
*corresponding author, E-mail: raelch@mek.dtu.dk

ABSTRACT

This study considers a recently proposed topology optimization based approach for designing photonic membrane cavities supporting a dipole cavity mode. Foremost, the study demonstrates that the approach is robust towards the choice of initial guess provided for the optimization problem, in the sense that near identical final designs are obtained for vastly different initial guesses. This finding suggests that the final designs are near-optimal under the given design constraints. Secondarily, by stopping the design procedure after the same fixed number of design iterations for all initial guesses, it shows that the designed photonic cavity is sensitive towards certain small perturbations of their geometry, stressing the need for utilizing robust optimization techniques and imposing fabrication conforming length-scales in the cavity geometries.

keywords: Purcell factor, cavities, quality factor, resonators, manufacturing resolution, topology optimization, inverse problems

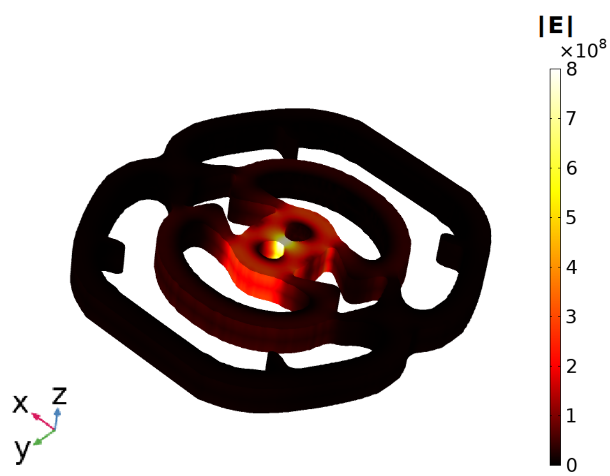

Figure 1: An optimized photonic cavity geometry. The electric field norm of the targeted mode at the resonant frequency is shown using the thermal color map.

Nanoengineering: Fabrication, Properties, Optics, Thin Films, and Devices XVI,
edited by Balaji Panchapakesan, André-Jean Attias, Proc. of SPIE Vol. 11089,
110890A · © 2019 SPIE · CCC code: 0277-786X/19/$21 · doi: 10.1117/12.2529099

1. INTRODUCTION

The design of high Purcell factor photonic cavities, i.e. cavities with large Q/V-ratios, has received a lot of attention over the last decades. Here Q denotes the quality factor of a given mode in the cavity and V the associated modal volume.[1–4] Photonic cavities composed of semi-conductor materials, capable of supporting highly spatio-temporally confined modes (high Q/V), as illustrated in Figure 1, are of great interest for a wide range of applications, including lasers,[5,6] sensors[7] and optomechanics.[8] Having the ability to design such structures at will, directly targeting a specific frequency, mode shape and characteristic cavity size is therefore potentially highly valuable. Further, having the ability to assure manufacturability of the designed cavity structure is paramount as design blueprints which are not manufacturable hold little to no practical value. A recently proposed approach[9] utilizing topology optimization coupled with advanced techniques for controlling the material phase length scales,[10,11] accomplishes exactly these goals.

In the present paper, we first outline the approach from[9] followed by a study demonstrating that the approach is robust towards the initial guess provided as the starting point for the optimization based design procedure. This study illustrates that the optimization based design approach avoids getting stuck in poorly performing local minima but instead is able to consistently identify a specific highly performing cavity structure independent of the provided initial guess. The geometry of the optimized design is instead only depending on the targeted frequency, resonant mode type, e.g. monopole, dipole, quadrupole; choice of design domain size; of the constituent material and of the imposed material phase length-scale.

2. METHOD

The goal of the design procedure proposed in[9] is to create and optimize high Purcell factor photonic membrane cavities supporting a dipole mode while adhering to user specified fabrication constraints. The physics is modelled in the complex frequency domain, rather than as an eigenvalue problem, using the approach proposed in.[12] Here a dipole source with a specified in-plane orientation is introduced in the model to excite the desired mode. The physics is modelled under the time harmonic assumption using a vectorial partial differential equation derived from Maxwell's Equations with appropriate boundary conditions,

$$\nabla \times \frac{1}{\mu(\boldsymbol{x})} \nabla \times \boldsymbol{E}(\boldsymbol{x}) - \varepsilon(\boldsymbol{x}) \omega^2 \boldsymbol{E}(\boldsymbol{x}) = i\omega \boldsymbol{J}(\boldsymbol{x}). \tag{1}$$

Here $\boldsymbol{E}$ denotes the electric field, $\omega = 2\pi\nu$ the free-space angular frequency with ν being the frequency, ε denotes the electric permittivity and μ the magnetic permeability. $\boldsymbol{J}$ models the electric dipole source and i denotes the imaginary unit.

As a platform for designing the photonic membrane cavities, a model domain $\boldsymbol{\Omega} \in \mathbb{R}^3$ sketched in the left panel of Figure 2 is considered. The domain consists of an air-region (grey) with a design domain $\boldsymbol{\Omega}_\mathrm{d} \subset \boldsymbol{\Omega}$ at its centre. The photonic cavity under design occupies $\boldsymbol{\Omega}_\mathrm{d}$ with the dipole source placed at its centre (red dot). Due to the symmetry of the field pattern of the targeted dipole mode, the modelling may be simplified by imposing three symmetry planes in $\boldsymbol{\Omega}$, reducing the model domain to one eight of the total domain as illustrated in the right panel of Figure 2.

The symmetries are imposed through the use of appropriate boundary conditions based on the orientation of the dipole source. Perfect electric (PEC $\mathbf{n} \times \mathbf{E} = 0$), and magnetic (PMC $\mathbf{n} \times \mathbf{H} = 0$) conducting boundaries are introduced to enforce the symmetries as illustrated in the right panel of Figure 3. First order absorbing boundary conditions are imposed on the outer edges of $\boldsymbol{\Omega}$. The side length of $\boldsymbol{\Omega}_\mathrm{d}$ in the (x,y)-plane is denoted t and the characteristic size of the surrounding air-region d, as illustrated in the left panel of Figure 3. The height of the cavity membrane structure is denoted h.

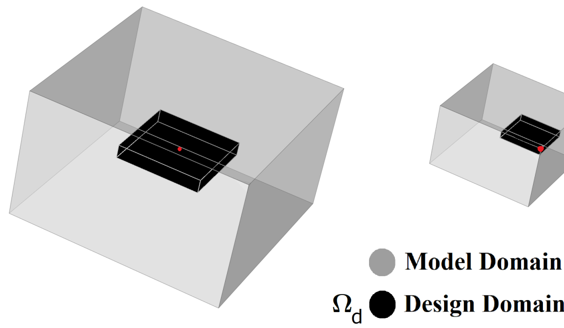

Figure 2: [Left] Sketch of the full modelling domain $\mathbf{\Omega}$ with the immersed design domain $\mathbf{\Omega}_{\mathrm{d}}$. [Right] Sketch of the reduced modelling and design domain after imposing threefold mirror symmetry.

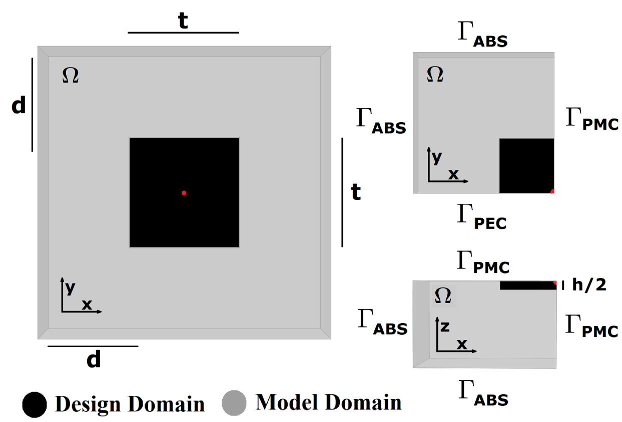

Figure 3: [Left] Top-down sketch of the full modelling and design domain with cavity side length $t = 3080$ nm and air region size $d = 1200$ nm. [Right] Symmetry-reduced modelling domain indicating the boundary conditions imposed accordingly and showing the membrane thickness $h = 250$ nm. $\Gamma_{\mathbf{ABS}}$: Absorbing boundary, $\Gamma_{\mathbf{PMC}}$: Perfectly magnetic conducting boundary, $\Gamma_{\mathbf{PEC}}$: Perfectly electric conducting boundary.

The photonic membrane cavity is taken to be of constant cross sectional geometry in the (x,y)-plane extruded to the appropriate height. The cross sectional geometry is then sought designed to maximize the quality of the cavity, measured as the Q/V-ratio for the targeted dipole mode (directly proportional to the local density of state for the dipole source). This design problem is recast as a constrained optimization problem and solved by density based topology optimization techniques[13,14] using the material interpolation proposed in.[15] Standard filtering and thresholding techniques are used to regularize the problem.[11,16]

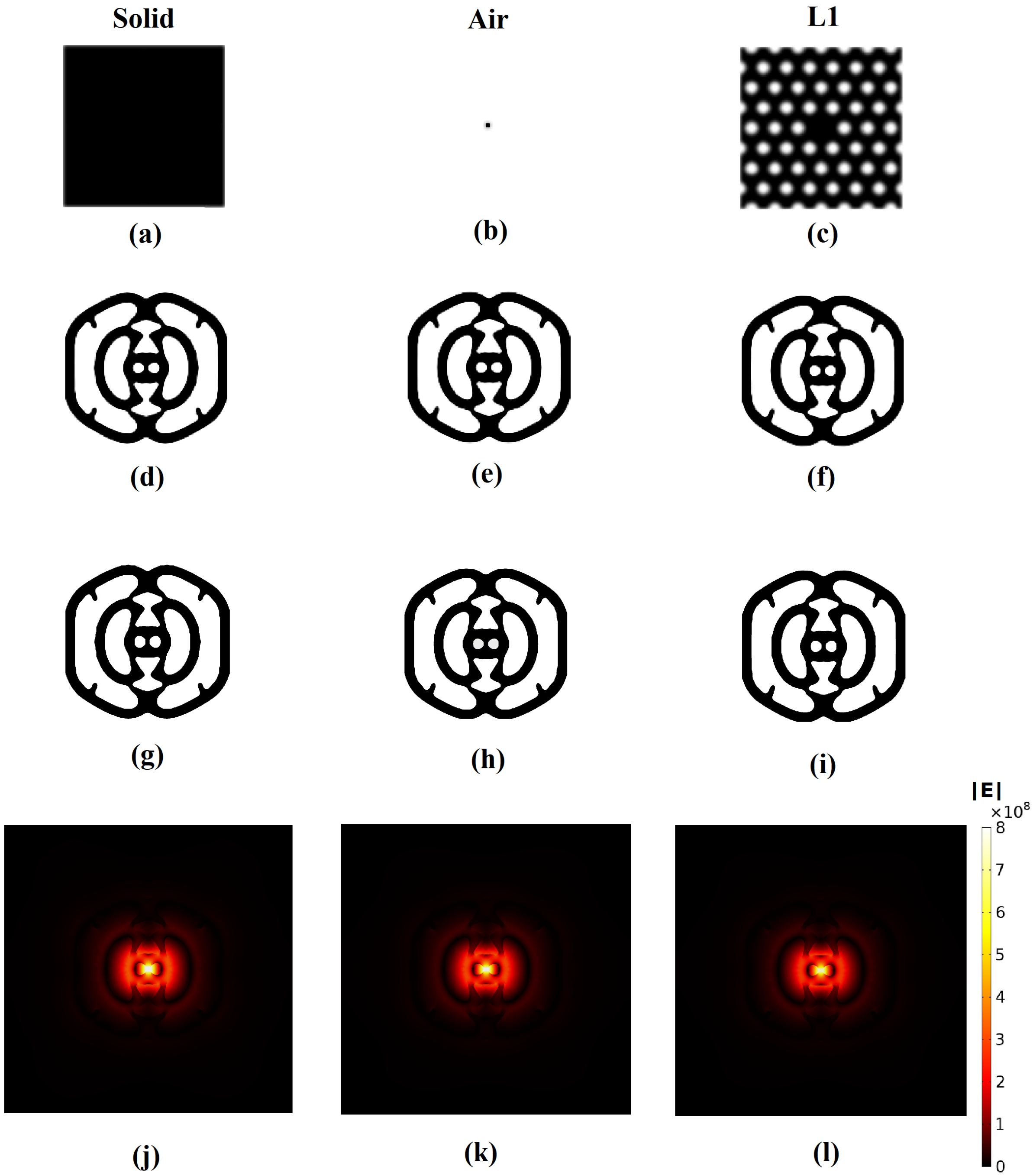

Figure 4: Images of (x,y)-plane cross sections of (a-c) the initial guesses, $\rho_{\text{ini}}(x, y)$, provided to the optimization algorithm, (d-f) the final material distributions, $\rho_{\text{final}}(x, y)$, resulting from the optimization procedure, (g-i) the final post processed design geometries and (j-l) the mode profile at the resonant frequency. The left column of panels reports data for the initial guess $\rho_{\text{ini}} = 1$. The middle column reports data for the initial guess $\rho_{\text{ini}} = 0$ except at the source position where material is placed. The right column reports data for the initial guess consisting of an L1-cavity in a classic photonic crystal structure.

Initial Guess	Air	L1	Solid
λ [nm]	≈ 1553	≈ 1559	≈ 1553
Q/V $\left[\left(\frac{n}{\lambda}\right)^3\right]$	≈ 22800	≈ 22400	≈ 23600

Table 1: Resonance wavelength and Q/V-value for the designs reported in Figure 4(g-i).

3. DISCUSSION

It is important to note that it is (almost) never possible to guarantee the global optimality of a solution to any non-convex optimization problem, without testing all possible permutations of the design variable values. That being said, this study shows that the final optimized cross sectional cavity geometry is independent on the initial guess provided to the optimization algorithm for the investigated problem setup. This demonstrates that the proposed approach is capable of identifying the same locally optimal, high quality, solution independent of initial guess, pointing to the robustness of the method in designing photonic membrane cavities.

For the example treated in this study, an InP ($n = 3.17$) membrane cavity embedded in air ($n = 1.00$) capable of supporting a dipolar mode at $\lambda = 1550$ nm with the dimensions reported in Figure 3, is sought designed. No length-scale nor geometric robustness is imposed in the design procedure. A fixed number of 3800 design iterations is used for all cases. Due to the choice of the number of iterations, the final designs are intentionally not completely identical[1], as a different number of iterations are needed to arrive at the locally optimal solution, depending on the initial guess. This fixed number of iterations is used to illustrate that small deviations in the final geometry may result in significant variations of the performance of the final design. This highlights the potential benefit of utilizing methods which improve the geometric robustness of the optimized designs as well as methods for imposing length-scales in the design, hereby supporting accurate fabrication of the final design blueprints to avoid small, yet important, geometric variations (as was done in[9]).

A number of different initial guesses are provided for the design procedure. Figure 4(a)-(c) shows initial guesses consisting of a solid slab of material filling the entire $\mathbf{\Omega}_\text{d}$; an empty $\mathbf{\Omega}_\text{d}$ outside of a small solid region around the dipole source which is kept fixed as solid for all cases; an L1-cavity inside a PhC-membrane slab in $\mathbf{\Omega}_\text{d}$. Starting from these initial guesses the design procedure is applied. The resulting final design fields, $\rho_{\text{final}}(x, y) \in [0, 1]$, are reported in 4(d)-(f). These panels clearly show that qualitatively similar final designs are obtained from the procedure. Meanwhile, if one looks closely at the panels it is possible to see small quantitative differences between the design fields, differences which disappears if the design procedure is allowed to run until convergence. In order to evaluate the performance of the final designs, clear InP/air designs are recovered from the final design fields, these are reported in Figure 4(g)-(i). The targeted dipole mode is computed for the final designs using COMSOL Multiphysics and the resulting $|\mathbf{E}|$-field in a slice in the (x,y)-plane at the centre of the membrane, reported in Figure 4(j)-(l). From the panels it is near-impossible to see any difference. Based on the computation of the dipole mode the excitation wavelength and the Q/V-value is computed for all three cases and the values reported in table 1.

From the table it is seen that despite the designs being visually near-indistinguishable on the macroscopic scale, the Q/V-values actually change by $\approx\ 5.1\%$ from "Solid" to "L1" due to the small geometric variations in the geometries on the order of ≈ 10 nm in some parts of the design and the order of ≈ 1 nm in other parts. A frequency shift from the targeted 1550 nm is likewise observed from the table. This shift is caused by the conversion of the design field in Figure 4(d)-(f) to the post processed perfect InP/Air smooth structures in Fig 4(g)-(i).

[1]They become identical if a sufficient number of design iterations are used.

4. CONCLUSION

This study demonstrates that the approach proposed in[9] is able to identify the same locally optimal solution independent of the investigated, vastly different, initial guesses. This shows that the method is robust towards the initial material distribution, further suggesting that the final design is near-optimal under the specific design constraints. Further it is demonstrated that the final design is sensitive to (certain) small geometry variations, which highlights the potential benefits of applying robust design techniques and imposing length-scales to conform with fabrication restrictions.

Acknowledgement

The authors acknowledge support from the Villum Centre of Excellence, NATEC (NAnophotonics for Terabit Communications) (Grant No. 8692) and from the Villum Investigator programme InnoTop (Interactive, Non-Linear, High-Resolution Topology Optimization).

References

[1] Akahane, Y., Asano, T., Song, B.-S., and Noda, S., "High-Q photonic nanocavity in a two-dimensional photonic crystal", Nature 425, 944 (2003).

[2] Wang, D., Yu, Z., Liu, Y., Guo, X., Shu, C., Zhou, S., and Zhang, J., "Ultrasmall modal volume and high Q factor optimization of a photonic crystal slab cavity", Journal of Optics 15, 125102, (2013).

[3] Choi, H., Heuck, M., and Englund, D., "Self-similar nanocavity design with ultrasmall mode volume for single-photon nonlinearities", Physical Review Letters 118, 223605, (2017).

[4] Hu, S., Khater, M., Salas-Montiel, R., Kratschmer, E., Engelmann, S., Green, W. M., and Weiss, S. M., "Experimental realization of deep-subwavelength confinement in dielectric optical resonators", Science Advances 4, eaat2355, (2018).

[5] Painter, O., Lee, R., Scherer, A., Yariv, A., O'brien, J., Dapkus, P., and Kim, I., "Two-dimensional photonic band-gap defect mode laser", Science 284, 1819–1821, (1999).

[6] Xue, W., Yu, Y., Ottaviano, L., Chen, Y., Semenova, E., Yvind, K., and Mørk, J., "Threshold characteristics of slow-light photonic crystal lasers", Physical Review Letters 116, 063901, (2016).

[7] Pitruzzello, G., and Krauss, T. F., "Photonic crystal resonances for sensing and imaging", Journal of Optics 20, 073004, (2018).

[8] Kippenberg, T. J., and Vahala, K. J., "Cavity optomechanics: Back-action at the mesoscale", Science 321, 1172–1176, (2008).

[9] Wang, F., Christiansen, R. E., Yu, Y., Mørk, J., and Sigmund, O., "Maximizing the quality factor to mode volume ratio for ultra-small photonic crystal cavities", Applied Physics Letters 113, 241101, (2018).

[10] Zhou, M., Lazarov, B. S., Wang, F., and Sigmund, O., "Minimum length scale in topology optimization by geometric constraints", Computer Methods in Applied Mechanics and Engineering 293, 266–282, (2015).

[11] Wang, F., Lazarov, B. S., and Sigmund, O., "On projection methods, convergence and robust formulations in topology optimization", Structural Multidisciplinary Optimization 43, 767–784, (2011).

[12] Liang, X., and Johnson, S. G., ”Formulation for scalable optimization of microcavities via the frequency-averaged local density of states”, Optical Express 21, 30812–30841, (2013).

[13] Jensen, J. S., and Sigmund, O., ”Topology optimization for nano-photonics”, Laser & Photonics Reviews 5, 308-321, (2011).

[14] Svanberg, K., ”The method of moving asymptotes - a new method for structural optimization”, International Journal For Numerical Methods in Engineering 24, 359–373, (1987).

[15] Christiansen, R. E., Vester-Petersen, J., Madsen, S. P., and Sigmund, O., ”A non-linear material interpolation for design of metallic nano-particles using topology optimization”, Computer Methods in Applied Mechanics and Engineering 343, 23–39, (2019).

[16] Guest, J. K., Prevost, J. H., Belytschko, T., ”Achieving minimum length scale in topology optimization using nodal design variables and projection functions”, International Journal For Numerical Methods in Engineering 61, 238–254, (2004).